Journal of Materials Chemistry C

Accepted Manuscript

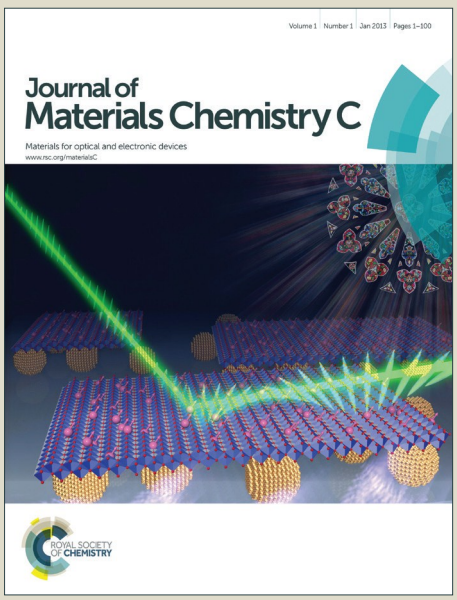

ROYAL SOCIETY OF CHEMISTRY

www.rsc.org/materialsC

Journal Name

ARTICLE

High-Efficiency Solution-Processed OLEDs Based on Cationic Ag_6Cu Heteroheptanuclear Cluster Complexes with Aromatic Acetylides

Received 00th January 20xx,
Accepted 00th January 20xx

DOI: 10.1039/x0xx00000x

www.rsc.org/

Liang-Jin Xu,[‡] Xu Zhang,[‡] Jin-Yun Wang and Zhong-Ning Chen*

We report herein the first use of phosphorescent copper(I)-silver(I) heterometallic complexes to achieve highly efficient electroluminescence. The trigonal prism arranged Ag_6Cu heteroheptanuclear alkynyl cluster complexes show intense phosphorescence in fluid solution, powder and film with quantum yields as high as 0.78. Complex **1** with 1-(tert-butyl)-4-ethynylbenzene ($HC{\equiv}CC_6H_4Bu^t$-4) shows reversible phosphorescence vaporchromism in respose to THF or $CHCl_3$. The phosphorescent emission exhibits an obvious blue-shift from 580 nm to 530 nm for THF and to 538 nm for $CHCl_3$ with a remarkable luminescence change from bright yellow to green. As demonstrated experimentally and theoretically, the phosphorescence originates from $^3[\pi$ (aromatic acetylide) $\rightarrow$ s/p (Ag_6Cu)] ^{3}LMCT and Ag_6Cu cluster centered $^3[d{\rightarrow}s/p]$ triplet states. Taking advantage of doped light-emitting layer of 57% TCTA : 28% OXD-7 : 15% Ag_6Cu complex with hole-transporting TCTA and electron-transporting OXD-7 as blended host, solution-processed OLEDs gave highly efficient electroluminescence with current efficiency (CE) of 42.5 cd/A and external quantum efficiency (EQE) of 13.9% at low voltage (4.5 V) and practical brightness (184 cd/m^2).

Introduction

In view of immense application of organic electroluminescence in display and lighting fields, it is urgently needed to develop environment-benign, low-cost organo-metal compounds to replace metal complexes with rare elements such as Ir,[1] Pt,[2] Au,[3] and Os[4] etc, which have been vigorously investigated as phosphorescent dopants in organic light-emitting diodes (OLEDs). Recently, lead(II) halide perovskite complexes have been utilized as light-emitting materials for electroluminescence,[5] in which external quantum efficiency (EQE) is not only still low (< 10%), but lead(II) species is also not environment-benign. By comparison, luminescent zinc(II) complexes are better candidates as light-emitting materials to achieve efficient electroluminescence.[6]

Since a copper(I) complex was firstly utilized as phosphorescent material to fabricate single-layer device ITO/Cu_4:PVK/Al with external quantum efficiency of 0.1%,[7a] mononuclear and binuclear copper(I) complexes have been boomingly explored as light-emitting materials for efficient electroluminescence.[7-10] Nevertheless, low chemical stability of copper(I) complexes in solution and at relatively high temperature remains an problem for the fabrication of devices through solution process or thermal evaporation deposition. To address this issue, one of the possible strategies is to design heterometallic cluster structures with copper(I) ion encapsulated by other metal ions through significant metalophilic contact. In this regard, copper(I)-silver(I) heterometallic cluster complexes with copper(I) embraced by silver(I) atoms are ideal candidates for developing environment-benign and low-cost electroluminescent devices. Unfortunately, among a limited number of copper(I)-silver(I) heterometallic complexes, most of them are weakly emissive at ambient condition with low quantum yields.[11]

Taking advantage of rigid tris(diphenylphosphino)methane ($CH(PPh_2)_3$) as a supported ligand, we are able to access highly phosphorescent Ag_6Cu heteroheptanuclear alkynyl cluster complexes (Scheme 1) with quantum yields of 0.53 in fluid CH_2Cl_2 and 0.78 in powder state. Since these strongly phosphorescent Ag_6Cu species are not only photo-chemically and thermally stable, but also soluble in organic solvents such as CH_2Cl_2 and $CHCl_3$ etc, they are ideal phosphorescent dopants for solution-processed OLEDs, thus achieving highly efficient electroluminescence with current efficiency of 42.5 cd/A and EQE as high as 13.9% at a low voltage (4.5 V).

Results and discussion

Ag_6Cu complex **1** (Scheme 1) was first isolated from the reaction of $CH(PPh_2)_3$, polymeric $(AgC{\equiv}CC_6H_4Bu^t\text{-}4)_n$ and $[Cu(MeCN)_4](ClO_4)$ in low yield (< 10%), in which diphenylphosphinic acid ($Ph_2P(O)OH$) resulted probably from the decomposition of a small portion of $CH(PPh_2)_3$. In order to acquire Ag_6Cu complexes in reasonable yields, complexes **1**–**5** (Scheme 1) were successfully reproduced by the reactions of

State Key Laboratory of Structural Chemistry, Fujian Institute of Research on the Structure of Matter, Chinese Academy of Sciences, Fuzhou, Fujian 350002, China

† Electronic Supplementary Information (ESI) available: Tables and figures giving additional photoluminescence, electroluminescence and TD-DFT results, and X-ray crystallographic files in CIF format for **1**·6CH_2Cl_2 (CCDC 1409777) and **5**·3CH_2Cl_2 (CCDC 1409778). See DOI: 10.1039/x0xx00000x

‡ These authors contributed equally.

$CH(PPh_2)_3$, $(AgC{\equiv}CC_6H_4R\text{-}4)_n$, $Ph_2P(O)OH/Ph_2P(S)SH$, and $[Cu(MeCN)_4](ClO_4)$ in a 2 : 6 : 3 : 1 molar ratio. Diffusion of petroleum ether onto CH_2Cl_2 solutions in a few days afforded well-shaped crystals in 47%–65% yield. Attempt to prepare Ag_6Cu complexes directly using $[Ag(tht)](ClO_4)$ and $HC{\equiv}CC_6H_4R\text{-}4$ as the starting materials in place of $(AgC{\equiv}CC_6H_4Bu^t\text{-}4)_n$ was unattained whether a base (triethylamine) was used or not. To clarify the influence of organic phosphate on the luminescent properties of Ag_6Cu species, complex **5** was accordingly synthesized using diphenyldithiophosphonic acid ($Ph_2P(S)SH$) instead of diphenylphosphinic acid ($Ph_2P(O)OH$).

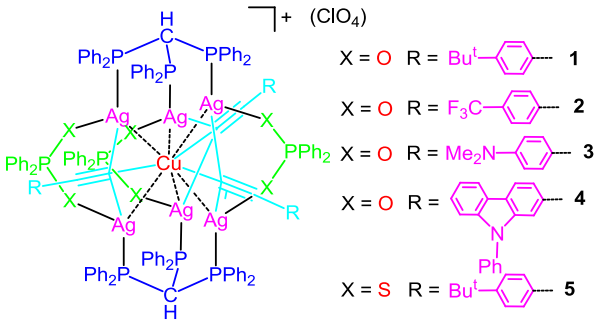

Scheme 1. Ag_6Cu heteroheptanuclear cluster complexes **1**–**5**.

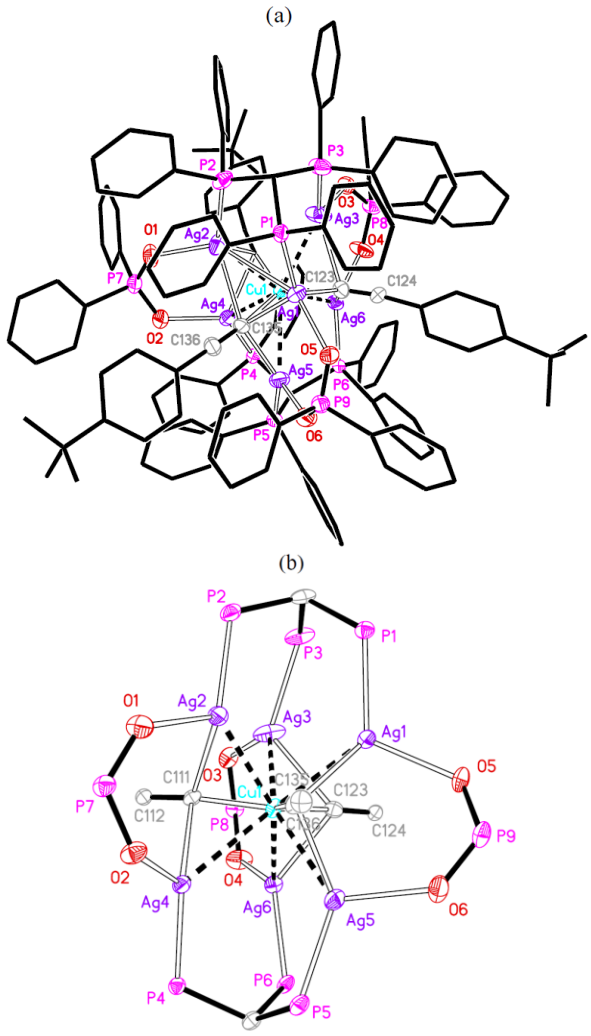

Figure 1. (a) A perspective view of Ag_6Cu complex cation of **1**. (b) ORTEP drawing of complex cation of **1**, showing 30% thermal ellipsoids. Phenyl rings on phosphorus atoms and acetylides are omitted for clarity. Selected interatomic distances (Å) and bond angles (°): Ag1-Cu1 2.6586(10), Ag2-Cu1 2.6312(10), Ag3-Cu1 2.7099(11), Ag4-Cu1 2.8146(11), Ag5-Cu1 2.8087(10), Ag6-Cu1 2.6803(10), Cu1-C123 1.959(7), Ag1-C123 2.649(7), Ag3-C123 2.470(8), Ag6-C123 2.364(7); C111-Cu1-C123 122.4(3), C111-Cu1-C135 116.7(3), C123-Cu1-C135 120.1(3).

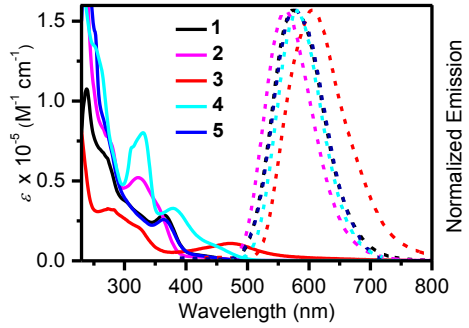

Figure 2. The UV–Vis absorption and emission spectra of complexes **1**–**5** in fluid CH_2Cl_2 (2×10^{-5} M) at ambient temperature.

Compounds **1**·$6CH_2Cl_2$ (Figure 1) and **5**·$3CH_2Cl_2$ (Figure S1 in ESI) were determined by X-ray crystallography. As shown in Figure 1 and Figure S1, the Ag_6Cu cluster structure results likely from incorporating two cationic $[HC(Ph_2P{-}Ag)_3]^{3+}$ moieties to one dianionic $[Cu(C{\equiv}CC_6H_4Bu^t\text{-}4)_3]^{2-}$ through the formation of six Ag–acetylide bonds and six Ag–Cu contacts. The Ag_6Cu cluster is further stabilized by three bridging anionic $Ph_2P(O)O$ (complex **1**) or $Ph_2P(S)S$ (complex **5**) through Ag-O-PPh_2-O-Ag or Ag-S-PPh_2-S-Ag linkages. The Ag_6Cu cluster exhibits a triangular prismatic geometry with copper(I) atom at the center of this prism. In fact, the Ag_6Cu cluster cations of **1** and **5** display a pseudo C_3 and C_3 rotational symmetry, respectively. The central copper(I) atom is encapsulated by six silver(I) atoms through Ag–Cu contact as well as three σ-bound arylacetylides. The Ag···Cu distances are in the range 2.6312(10)–2.8146(11) Å and much shorter than the sum of van der Waals radii of Ag and Cu atoms (3.12 Å), implying the presence of significant Ag–Cu metallophilic interaction.[11] In contrast, the Ag···Ag distances are mostly longer than 3.35 Å, the sum of van der Waals radii of two Ag atoms, suggesting quite weak Ag–Ag contact.

The acetylides adopt μ_4-η^1(Cu),η^1(Ag),η^1(Ag),η^1(Ag) and μ_3-η^1(Cu),η^1(Ag),η^1(Ag) bonding mode for **1** whereas μ_3-η^1(Cu),η^1(Ag),η^2(Ag) asymmetric fashion for **5**, in which the Cu–C≡C σ-coordination is quasi-linear with Cu–C≡C angles being 163-171° whereas the Ag–C≡C linkages are curve. The three P donors of $CH(PPh_2)_3$ are bound to three Ag centers whereas diphenylphosphinate or diphenylphosphinodithioate bridges two silver(I) through Ag-O-P-O-Ag or Ag-S-P-S-Ag linkage. The copper(I) atom is coordinated by three σ-bound acetylide C donors to give an approximate triangular planar environment. The $C_{acetylide}$-Cu-$C_{acetylide}$ angles are 116.7(3), 120.1(3) and 122.4(3)° for **1** and 119.89(2)° for **5**. The silver(I) center is surrounded by CPO/C_2PO or CPS donors to form a distorted triangular planar or tetrahedral geometry.

The UV–Vis electronic absorption spectra (Figure 2) of complexes **1**–**5** exhibit intense absorption bands at ca. 220–350 nm and low-energy shoulder peaks tailing to 580 nm. The high-energy bands are mainly due to aromatic acetylides and $CH(PPh_2)_3$ with some metal-participated character. The broad low-energy bands longer than 350 nm are ascribed to charge transfer states mixed with Ag_6Cu cluster centered character.

Table 1. The Photoluminescent Data for Ag_6Cu Cluster Complexes **1**–**5.**

compound	state[a]	λ_{em} (nm)	τ_{em} (μs)	Φ_{em}[b]	k_r (s^{-1})
1	CH_2Cl_2	575	1.46	0.20	1.38×10^5
	powder	580	4.63	0.78	1.68×10^5
	film	562	9.59	0.43	4.48×10^4
2	CH_2Cl_2	561	2.16	0.25	1.14×10^5
	powder	573	3.32	0.45	1.36×10^5
3	CH_2Cl_2	605	0.46	0.019	4.13×10^4
	powder	634	1.27	0.059	4.65×10^4
4	CH_2Cl_2	581	6.49	0.53	8.19×10^4
	powder	585	4.69	0.56	1.19×10^5
	film	571	5.70	0.45	7.93×10^4
5	CH_2Cl_2	578	1.63	0.19	1.13×10^5
	powder	557	2.94	0.59	2.00×10^5

[a] The film consists of 57% TCTA, 28% OXD-7 and 15% Ag_6Cu complex. [b] Solution quantum yields were measured in CH_2Cl_2 relative to that of $[Ru(bpy)_3](PF_6)_2$ in acetonitrile (Φ_{em} = 0.062). Absolute quantum yields of powders and films were measured using an integrating sphere. c) Radiative decay rate $k_r = \Phi_{em}/\tau$.

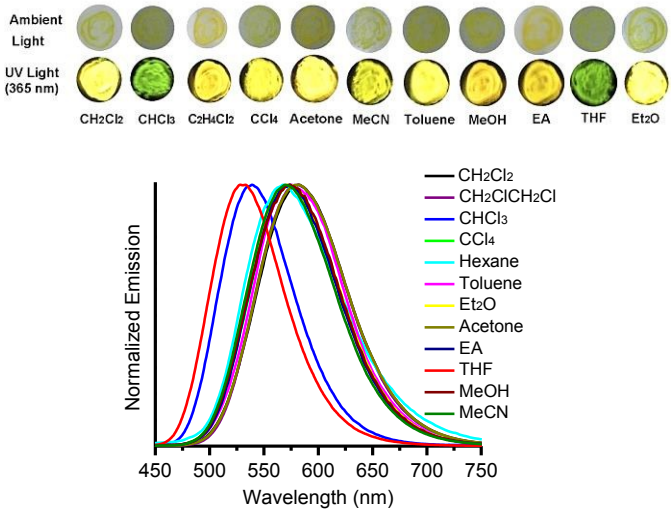

Figure 3. The photographic images (top) of **1** deposited on quartz slices upon exposure to selected organic vapors under ambient light and UV light irradiation (365 nm) and the emission spectra (bottom) of **1** upon exposure to various VOC vapors.

Upon irradiation at λ_{ex} > 300 nm, complexes **1–5** are strongly luminescent at ambient condition with quantum yields as high as 0.53 in fluid CH_2Cl_2 and 0.78 in powder state (Table 1). The emissive quantum yields are much higher than those of other Ag-Cu heterometallic cluster complexes (< 0.10 in solution),[11] ascribed to quite rigid and stable Ag_6Cu cluster structures consolidated by bridging $CH(PPh_2)_3$, $C{\equiv}CC_6H_4R$-4, and $Ph_2P(O)O/Ph_2P(S)$. The radiative decay rates lie in 10^4 s^{-1} to 10^5 s^{-1} (Table 1), much larger than those of other Ag-Cu heteronuclear complexes (ca. 10^3 s^{-1})[11c] and comparable to some highly emissive copper(I) complexes.[6-10,12,13] Large Stokes' shifts with microsecond range of emissive lifetimes indicate a triplet state parentage. It is noteworthy that the phosphorescence in fluid CH_2Cl_2 is hardly quenched by O_2 because the Ag_6Cu cluster core of complexes **1–5** is effectively shielded by external organic ligands. Upon lowering the temperature to 77 K, the emission spectra show obvious blue-shift (Figures S5 and S6) in contrast to red-shift in copper(I) complexes with thermally activated delayed fluorescence.[12,13]

Relative to that of complex **1** (λ_{em} = 575 nm), the emission maximum shows a distinct blue-shift for complex **2** (λ_{em} = 561 nm) whereas a large red-shift for complex **3** (λ_{em} = 605 nm) in fluid CH_2Cl_2. Such a spectral shift trend accords well with a lower lying HOMO (mainly π orbital of arylacetylide) and a larger HOMO-LUMO gap for **2** with electron-accepting CF_3 whereas a higher lying HOMO and a narrower HOMO-LUMO gap for **3** with electron-donating NMe_2. Both the absorption and emission bands of **5** (λ_{em} = 578 nm) are comparable to those of **1** (λ_{em} = 575 nm), implying the use of $Ph_2P(S)SH$ in place of $Ph_2P(O)OH$ exerts inappreciable influence on the photophysical feature.

Complexes **1**–**5** are highly phosphorescent in solid states. Interestingly, when desolvate species **1** (λ_{em} = 580 nm) is exposed to the vapor of THF or $CHCl_3$, the emission maximum shows a remarkable blue-shift to 530 nm for THF and 538 nm for $CHCl_3$. The photographs in Figure 3 show naked-eye perceivable luminescence conversion from bright yellow to green upon exposure to THF or $CHCl_3$ vapor. This luminescence vaporchromic process is totally reversible and the emission spectrum could be reverted to the one in original state (λ_{em} = 580 nm) upon exposure of the sample into other organic vapors such as CH_2Cl_2, acetone, MeOH and MeCN etc. It has been shown that luminescence vaporchromism in metal complexes originates most likely either from variation in metal-solvent bonding (intramolecular) or change in molecular packing due to formation/disruption of intermolecular metal-metal, π-π or hydrogen bonding interaction.[14,15] Since luminescence vaporchromic behavior is not observed for complexes **2**–**5**, it is likely that luminescence vaporchromism of complex **1** is relevant to the variation in intermolecular interaction perturbed by THF or $CHCl_3$ vapor.

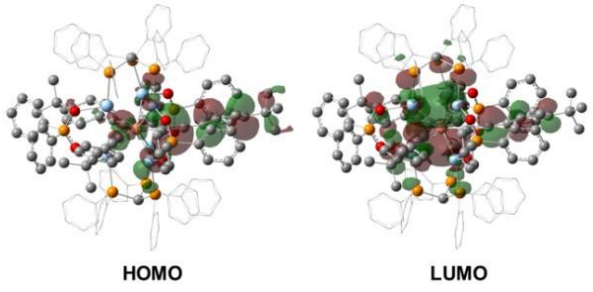

Figure 4. The HOMO and LUMO of complex **1**, resulting from TD-DFT studies for the triplet state geometry.

TD-DFT computational studies on complex **1** show that the HOMO (Figure 4) is primarily distributed to aromatic acetylide (65.0%) and Ag_6Cu cluster core (27.4%) and the LUMO is mainly populated at A_6Cu cluster core (74.4% with 37.8% at Cu center and 36.6% at Ag center). The phosphorescence arises mainly from $^3[\pi\ (C{\equiv}CR) \rightarrow s/p\ (Ag_6Cu)]$ ^{3}LMCT and Ag_6Cu cluster centered $^3[d \rightarrow s/p]$ triplet states. As shown in Figure 4, diphenylphosphinate is little involved in HOMO and LUMO so that $Ph_2P(O)O$ or $Ph_2P(S)S$ plays only a role in stabilizing Ag_6Cu cluster structure with little contribution to optical character, coinciding with their similar emissive properties between compounds **1** and **5**.

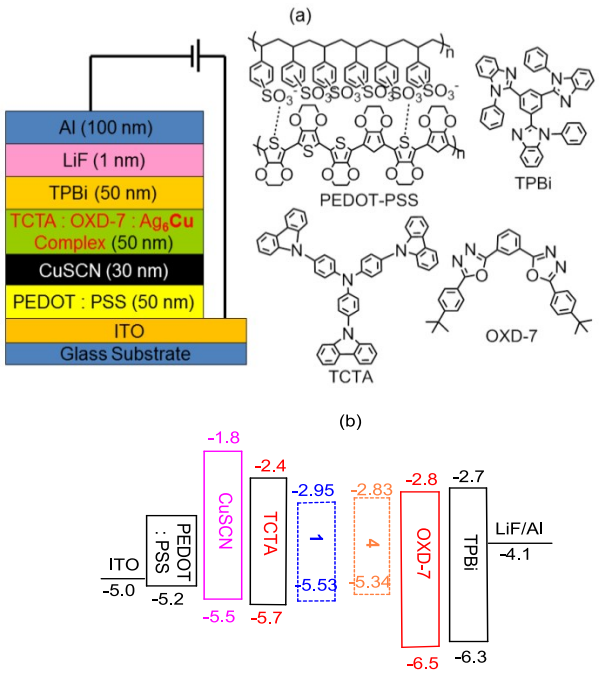

Scheme 2. The diagram of the device together with organic materials (a) and energy level diagrams (b). The HOMO and LUMO levels of complexes **1** and **4** were estimated by oxidation potentials of cyclic voltammetry and optical band gaps.

As displayed in Figure 4, an obvious spatial overlapping of HOMO and LUMO implies a large exchange integral and thus a large singlet–triplet energy gap $\Delta E(S_1{-}T_1)$.[12] In fact, the $\Delta E(S_1{-}T_1)$ is estimated as 1.03 eV (8307 cm^{-1}), which is much higher than those found in copper(I) complexes (< 0.3 eV) with thermally activated delayed fluorescence.[13] The spatial superposition between HOMO and LUMO also results in a large electric dipole moment as reflected by considerable oscillator strength (0.1006) of the transition $S_0 \rightarrow S_1$, corresponding to the measured low-energy band (Figure 2) with the maximum at 364 nm (ε = 28650 M^{-1} cm^{-1}) due to ^{1}LMCT state. On the other hand, small energy separation (0.01 eV) between HOMO and HOMO−1 involving different d orbitals implies effective mixing of HOMO−1→LUMO singlet state to HOMO→LUMO lowest triplet state (T_1) through strong spin-orbit coupling (SOC).[12] Intersystem crossing (ISC) from the singlet state S_1 to triplet state T_1 is thus highly facilitated so that complex **1** gives a short emission decay time of excited triplet state (1.49 μs in fluid CH_2Cl_2 and 4.63 μs in powder), which is favorable for highly efficient electroluminescence.

Since highly phosphorescent cationic Ag_6Cu cluster complexes show favorable thermal (stable at 300 °C, Figure S11) and photochemical stability and good solubility in organic solvents, they are ideal emitting materials for solution-processed OLEDs. Compounds **1** and **4** were selected as phosphorescent dopants to fabricate devices (Scheme 2). Water-soluble PEDOT : PSS was used as hole-injection layer. Semiconductor CuSCN was chosen as a hole-transporting layer through spin-coating in diethyl sulfide. Phosphorescent Ag_6Cu complex **1** or **4** doped to mixed host composed of a hole-transporting host and an electron-transporting host was spin-coated in CH_2Cl_2 over CuSCN layer to form light-emitting layer. The devices were optimized by changing blending ratio between a hole-transport type and an electron-transport type host, doping weight percentage of phosphorescent Ag_6Cu species and electron-transporting/hole-blocking layer.

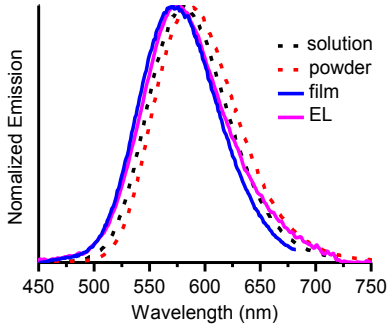

Figure 5. The photoluminescent spectra of complex **4** in fluid CH_2Cl_2, powder, and film composed of 57% TCTA, 28% OXD7 and 15% complex **4** together with the electroluminescent spectrum of device.

The use of hole-transporting TCTA (tris(4-(9H-carbazol-9-yl)phenyl)amine) and electron-transporting OXD-7 (1,3-bis(5-(4-(tert-butyl)phenyl)-1,3,4-oxadiazol-2-yl)benzene) in 2 : 1 weight ratio as mixed host gave better device performance. The doping concentration *vs* EQE (Figure S10) indicated that 15% Ag_6Cu complex doped to mixed host of TCTA (57%) and OXD-7 (28%) gave rise to the highest electroluminescent efficiency. Based on a four-layer device configuration ITO / PEDOT : PSS (50 nm) / CuSCN (30 nm) / 57% TCTA : 28% OXD-7 : 15% Ag_6Cu complex (50 nm) / TPBi (50 nm) / LiF (1 nm) / Al (100 nm) as shown in Scheme 2, solution-processed devices gave optimal electroluminescence performance as listed in Table 3. The turn-on voltage at 1 cd/m^2 is only 3.5 V for complex **1** and 3.4 V for complex **4**, comparable to those in the devices of iridium(III) or platinum(II) complexes by thermal evaporation deposition.[1-4] The electroluminescent spectrum of complex **4** (573 nm, Figure 5) shows a little blue-shift relative to the emission spectrum in fluid CH_2Cl_2 (581 nm) or powder (585 nm), but coincides well with that in doping film (571 nm) of TCTA (57%) : OXD-7 (28%) : complex **4** (15%), demonstrating that energy transfer is quite effective from mixed host to Ag_6Cu species so that the high-energy emission of mixed host is entirely quenched.

Journal Name

ARTICLE

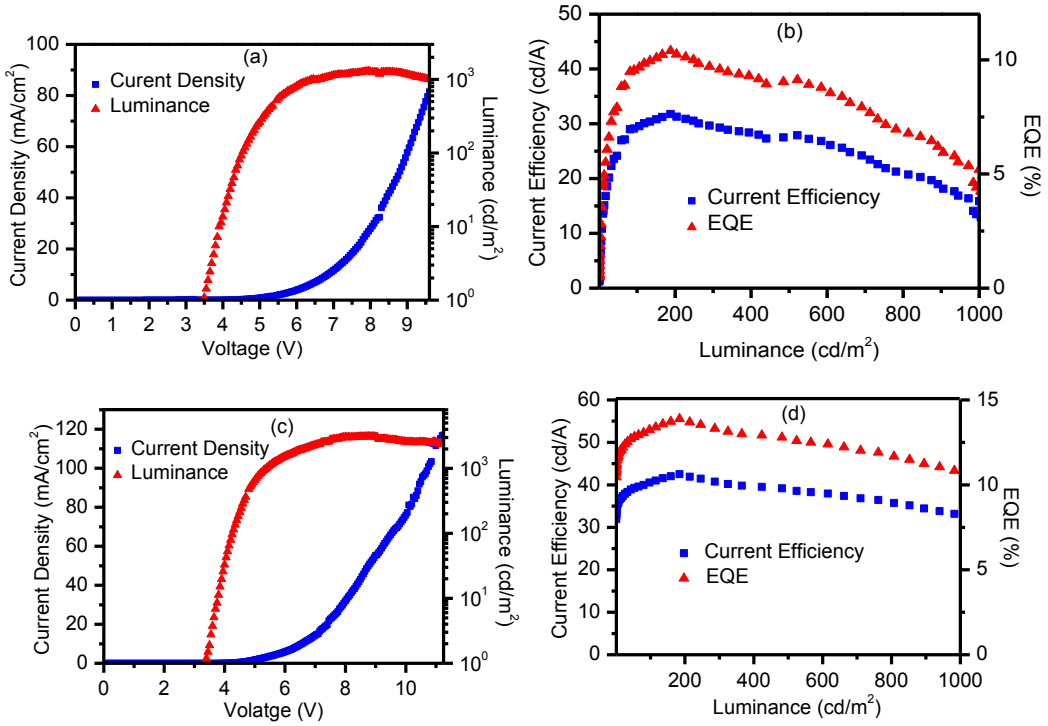

Figure 6. (a) Current density-voltage-luminance (J-V-L) characteristics of the device based on complex **1**. (b) Current efficiency/external quantum efficiency *vs* luminance for the device of complex **1**. (c) Current density-voltage-luminance (J-V-L) characteristics of the device based on complex **4**. (d) Current efficiency/external quantum efficiency *vs* luminance for the device of complex **4**.

Table 3. The Electroluminescent Data for Phosphorescent Complexes **1** and **4**.

complex	λ_{EL} (nm)	V_{on}[a] (V)	*CE* (cd/A)	*PE* (lm/W)	*EQE* (%)
1	565	3.5	31.8[b]	20.8[b]	10.4[b]
100 cd/m^2 (4.6V)			29.6	20.4	9.7
500 cd/m^2 (5.4 V)			27.9	16.1	9.1
4	573	3.4	42.5[c]	30.0[c]	13.9[c]
100 cd/m^2 (4.3 V)			40.6	30.0	13.2
500 cd/m^2 (4.8 V)			39.1	25.6	12.8

[a] Turn-on voltage at 1 cd/m^2. [b] Maximum efficiency at voltage of 4.8 V and brightness of 188 cd/m^2. [c] Maximum efficiency at voltage of 4.5 V and brightness of 184 cd/m^2.

Figure 6 depicts current density-voltage-luminance (J-V-L) characteristics and current efficiency/external quantum efficiency *vs* luminance for the devices based on **1** and **4**. For complex **1**, the highest electroluminescent efficiency occurs at voltage of 4.8 V and brightness of 188 cd/m^2 with current efficiency (CE) of 31.8 cd/A, power efficiency (PE) of 20.8 lm/W and EQE of 10.4 %. For complex **4**, the largest efficiency occurs at voltage of 4.5 V and brightness of 184 cd/m^2 with CE of 42.5 cd/A, PE of 30.0 lm/W and EQE of 13.9%. As shown in Figure 5c, the efficiency roll-off for the device of complex **4** is slow with only 7.9% decrease of the EQE at 500 cd/m^2, a practical brightness for flat panel display. The higher electroluminescent efficiency of complex **4** than that of complex **1** is ascribed to hole-transporting carbazole groups in complex **4** that facilitate carrier migration and exciton recombination in device.

Conclusions

A series of cationic Ag_6Cu heteroheptanuclear cluster complexes supported by $CH(PPh_2)_3$ and bridging diphenylphosphinate/diphenylphosphinodithioate were prepared as highly phosphorescent dopants for solution-

processed OLEDs. The Ag_6Cu cluster shows a triangular prismatic geometry with the central copper(I) atom encapsulated by six silver(I) atoms through significant Ag–Cu contact. The silver(I)-copper(I) heterometallic cluster complexes display strong phosphorescence in solution, powder and doped film with emissive quantum yields as high as 0.78, arising primarily from Ag_6Cu cluster centered ^{3}[d → s/p] and ^{3}[π (aromatic acetylide) → s/p (Ag_6Cu)] ^{3}LMCT triplet states. Complex **1** with 1-(tert-butyl)-4-ethynylbenzene shows remarkable vaporchromic phosphorescence in response to THF or $CHCl_3$ vapour. With complex **4** as a phosphorescent dopant, Solution-processed OLEDs based on four-layer device configuration gave highly efficient electroluminescence with CE of 42.5 cd/A, PE of 30.0 lm/W and EQE of 13.9% at a low voltage (4.5 V).

Experimental

General Procedures and Materials. All synthetic operations were conducted under dry argon atmosphere using Schlenk techniques unless otherwise specified. The solvents were dried, distilled, and degassed prior to use except that those for spectroscopic measurements were of spectroscopic grade. The reagents tris(diphenylphosphino)methane ($CH(PPh_2)_3$), diphenylphosphinic acid ($Ph_2P(O)OH$), diphenyldithiophosphonic acid ($Ph_2P(S)SH$) and 1-(tert-butyl)-4-ethynylbenzene ($HC{\equiv}CC_6H_4Bu^t$-4) were commercially available. 1-Ethynyl-4-(trifluoromethyl)benzene ($HC{\equiv}CC_6H_4CF_3$-4), 4-dimethylaminophenylacetylene ($HC{\equiv}CC_6H_4NMe_2$-4) and 2-ethynyl-9-phenyl-9H-carbazole (HC≡C-2-Phcarb-9) were prepared by the literature procedures.[16] The polymeric metal aromatic acetylide compounds $(AgC{\equiv}CC_6H_4R\text{-}4)_n$ (R = Bu^t, CF_3, NMe_2) and $(AgC{\equiv}C\text{-}2\text{-}Phcarb\text{-}9)_n$ together with $[Cu(MeCN)_4](ClO_4)$ were obtained by the described methods.[17]

Caution: Silver aromatic acetylides and perchlorate salts are potentially explosive and should be handled with care and in small amounts.

$[Ag_6Cu\{CH(PPh_2)_3\}_2(Ph_2PO_2)_3(C{\equiv}CC_6H_4Bu^t\text{-}4)_3](ClO_4)$ (1). To a CH_2Cl_2 (30 mL) solution of $CH(PPh_2)_3$ (56.8 mg, 0.1 mmol) was added $(AgC{\equiv}CC_6H_4Bu^t\text{-}4)_n$ (79.5 mg, 0.3 mmol) with stirring at room temperature for 15 min. $[Cu(MeCN)_4](ClO_4)$ (16.4 mg, 0.05 mmol) was then added to the reaction mixture, followed by the addition of diphenylphosphinic acid (32.7 mg, 0.15 mmol). The solution became brilliant yellow upon stirring at room temperature for 4 h. Layering petroleum ether onto the concentrated solution afforded **1** as yellow crystals in a few days. Yield: 52% (94 mg). Anal. Calcd for $C_{146}H_{131}Ag_6ClCuO_{10}P_9{\cdot}6CH_2Cl_2$: C, 50.99; H, 4.03. Found: C, 50.74; H, 4.15. ESI-MS: *m/z* 2971.3 $[M\text{-}ClO_4]^+$. ^{1}H NMR (400 MHz, CD_2Cl_2, δ): 8.08-7.94 (m, 24H), 7.73-7.62 (m, 10H), 7.27-7.19 (m, 8H), 7.13-7.04 (m, 18H), 6.97 (t, 12H, *J* = 7.4 Hz), 6.31 (t, 24H, *J* = 7.4 Hz), 6.34-6.28 (m, 6H), 5.62-5.46 (m, 2H), 1.09 (s, 27H). ^{31}P NMR (161.97 MHz, CD_2Cl_2, δ): 21.5 (s, 3P, Ph_2PO_2), 12.0 (m, 6P, $CH(PPh_2)_3$, $J_{Ag\text{-}P}$ = 612 Hz, $J_{P\text{-}P}$ = 35 Hz). IR (KBr): 2016w (C≡C), 1097s (ClO_4).

$[Ag_6Cu\{CH(PPh_2)_3\}_2(Ph_2PO_2)_3(C{\equiv}CC_6H_4CF_3\text{-}4)_3](ClO_4)$ (2). The synthetic procedure is the same as that of **1** except using $(AgC{\equiv}CC_6H_4CF_3\text{-}4)_n$ instead of $(AgC{\equiv}CC_6H_4Bu^t\text{-}4)_n$. Yield: 64% (99 mg). Anal. Calcd for $C_{137}H_{104}Ag_6ClCuF_9O_{10}P_9$: C, 52.97; H, 3.37. Found: C, 52.78; H, 3.41. ESI-MS: *m/z* 3006.4 $[M\text{-}ClO_4]^+$. ^{1}H NMR (400 MHz, CD_2Cl_2, δ): 8.04-7.92 (m, 24H), 7.83-7.65 (m, 10H), 7.32-7.26 (m, 8H), 7.26-7.13 (m, 18H), 7.01 (t, 12H, *J* = 7.4 Hz), 6.70 (t, 24H, *J* = 7.4 Hz), 6.58-6.54 (m, 6H), 5.62-5.46 (m, 2H). ^{31}P NMR (161.97 MHz, CD_2Cl_2, δ): 22.4 (s, 3P, Ph_2PO_2), 13.3 (m, 6P, $CH(PPh_2)_3$, $J_{Ag\text{-}P}$ = 571 Hz, $J_{P\text{-}P}$ = 35 Hz). IR (KBr): 2041w (C≡C), 1097s (ClO_4).

$[Ag_6Cu\{CH(PPh_2)_3\}_2(Ph_2PO_2)_3(C{\equiv}CC_6H_4NMe_2\text{-}4)_3](ClO_4)$ (3). The synthetic procedure is the same as that of **1** except using $(AgC{\equiv}CC_6H_4NMe_2\text{-}4)_n$ instead of $(AgC{\equiv}CC_6H_4Bu^t\text{-}4)_n$. Yield: 58% (88 mg). Anal. Calcd for $C_{140}H_{122}Ag_6ClCuN_3O_{10}P_9$: C, 55.47; H, 4.06; N, 1.39. Found: C, 55.76; H, 3.99; N, 1.32. ESI-MS: *m/z* 2931.8 $[M\text{-}ClO_4]^+$. ^{1}H NMR (400 MHz, CD_2Cl_2, δ): 8.16-8.05 (m, 24H), 7.87-7.70 (m, 10H), 7.63-7.52 (m, 8H), 7.13-7.00 (m, 18H), 6.87 (t, 12H, *J* = 7.4 Hz), 6.67 (t, 24H, *J* = 7.4 Hz), 6.32-6.19 (m, 6H), 5.56-5.40 (m, 2H), 2.91 (s, 18H). ^{31}P NMR (161.97 MHz, CD_2Cl_2, δ): 21.7 (s, 3P, Ph_2PO_2), 12.9 (m, 6P, $CH(PPh_2)_3$, $J_{Ag\text{-}P}$ = 603 Hz, $J_{P\text{-}P}$ = 36 Hz). IR (KBr): 1992w (C≡C), 1096s (ClO_4).

$[Ag_6Cu\{CH(PPh_2)_3\}_2(Ph_2PO_2)_3(C{\equiv}C\text{-}2\text{-}Phcarb\text{-}9)_3](ClO_4)$ (4). The synthetic procedure is the same as that of **1** except using $(AgC{\equiv}C\text{-}2\text{-}Phcarb\text{-}9)_n$ instead of $(AgC{\equiv}CC_6H_4Bu^t\text{-}4)_n$. Yield: 65% (110 mg). Anal. Calcd for $C_{170}H_{128}Ag_6ClCuN_3O_{10}P_9$: C, 60.09; H, 3.80, N, 1.24; Found: C, 59.91; H, 3.70; N, 1.37. ESI-MS: *m/z* 3297.0 $[M\text{-}ClO_4]^+$. ^{1}H NMR (400 MHz, CD_2Cl_2, δ): 8.10-7.98 (m, 30H), 7.75-7.67 (m, 14H), 7.29-7.23 (m, 8H), 7.16-7.09 (m, 22H), 7.00 (t, 16H, *J* = 6.8 Hz), 6.75-6.63 (m, 30H), 6.34 (d, 6H, *J* = 8.6Hz), 5.63-5.52 (m, 2H). ^{31}P NMR (161.97 MHz, CD_2Cl_2, δ): 21.5 (s, 3P, Ph_2PO_2), 12.0 (m, 6P, $CH(PPh_2)_3$, $J_{Ag\text{-}P}$ = 561 Hz, $J_{P\text{-}P}$ = 36 Hz). IR (KBr): 2011w (C≡C), 1095s (ClO_4).

$[Ag_6Cu\{CH(PPh_2)_3\}_2(Ph_2PS_2)_3(C{\equiv}CC_6H_4Bu^t\text{-}4)_3](ClO_4)$ (5). The synthetic procedure is the same as that of **1** except using diphenylphosphinodithioic acid instead of diphenylphosphinic acid. Yield: 43% (74 mg). Anal. Calcd for $C_{146}H_{131}Ag_6ClCuO_4P_9S_6{\cdot}3CH_2Cl_2$: C, 52.30; H, 4.04. Found: C, 52.13; H, 4.12. ESI-MS: *m/z* 3067.1 $[M\text{-}ClO_4]^+$. ^{1}H NMR (400 MHz, CD_2Cl_2, δ): 8.07-7.91 (m, 24H), 7.71-7.63 (m, 10H), 7.26-7.14 (m, 8H), 7.12-7.01 (m, 18H), 6.97 (t, 12H, *J* = 7.4 Hz), 6.64 (t, 24H, *J* = 7.4 Hz), 6.35-6.27 (m, 6H), 5.61-5.42 (m, 2H), 1.08 (s, 27H). ^{31}P NMR (161.97 MHz, CD_2Cl_2, δ): 21.6 (s, 3P, Ph_2PO_2), 11.7 (m, 6P, $CH(PPh_2)_3$, $J_{Ag\text{-}P}$ = 630 Hz, $J_{P\text{-}P}$ = 35 Hz). IR (KBr): 2017w (C≡C), 1097s (ClO_4).

Physical Measurements. The ^{1}H and ^{31}P NMR spectra were measured on a Bruker Auance III 400 spectrometer with $SiMe_4$ as the internal reference and H_3PO_4 as the external reference, respectively. Electrospay ion mass spectra (ESI-MS) were performed on a Finnigan LCQ mass spectrometer using dichloromethane-methanol as the mobile phase. Elemental analyses (C, H, N) were recorded on a Perkin-Elmer model 240C automatic instrument. UV–Vis absorption spectra were measured on a Perkin-Elmer Lambda 35 UV–Vis spectrometer. IR spectra were recorded on a Magna 750 FT-IR spectrophotometer with KBr pellets. The emission and excitation spectra together with the emissive lifetimes in solid states and degassed solutions were measured on Edinburgh FLS920 fluorescence spectrometer. The emission quantum

yield (Φ_{em}) in degassed dichloromethane solution at room temperature was calculated by $\Phi_s = \Phi_r(B_r/B_s)(n_s/n_r)^2(D_s/D_r)$ using $[Ru(bpy)_3](PF_6)_2$ in acetonitrile as the standard (Φ_{em} = 0.062),[18] where the subscripts r and s denote reference standard and the sample solution, respectively, and n, D and Φ are the refractive index of the solvents, the integrated intensity and the luminscence quantum yield, respectively. The quantity B is calculated by $B = 1\text{-}10^{-AL}$, where A is the absorbance at the excitation wavelength and L is the optical path length. The solid-state quantum yields of powder samples in sealed quartz cuvettes and films spin-coated in quartz substrates were determined by the integrating sphere (142 mm in diameter) using Edinburgh FLS920 Spectrofluorophotometer. Luminescence vapochromic experiments were performed upon sufficient exposure of the quartz slices to various saturated VOC vapors at ambient temperature for 5–10 min.

Crystal Structural Determination. Crystals of **1**·$6CH_2Cl_2$ and **4**·$3CH_2Cl_2$ were obtained by layering petroleum ether onto the CH_2Cl_2 solutions of **1** and **4**, respectively. Data collection was performed on Saturn70 CCD diffractometer by the ω scan technique at room temperature using graphite-monochromated Mo-Ka (λ = 0.71073 Å) radiation. The CrystalClear software package was used for data reduction and empirical absorption correction. The structures were solved by direct methods. The heavy atoms were located from E-map, and the rest of the non-hydrogen atoms were found in subsequent Fourier maps. All non-hydrogen atoms were refined anisotropically, while the hydrogen atoms were generated geometrically and refined with isotropic thermal parameters. The structures were refined on F^2 by full-matrix least-square methods using the SHELXTL–97 program package.[19] In the crystal of **4**·$3CH_2Cl_2$, the unit cell contains 24 dichloromethane molecules which have been treated as a diffuse contribution to the overall scattering without specific atom positions by SQUEEZE/PLATON.

Device Fabrication and Characterization. ITO substrates were cleaned by sonication in deionized water, acetone, and isopropanol followed by UV-ozone treatment for 15 min. PEDOT : PSS was filtered through a 0.22 μ m filter and spin-coated at 3000 rpm on the pre-cleaned substrates, and dried at 140 °C for 20 min to give a 50 nm thick film. CuSCN dissolved in diethyl sulfide at the concentration of 10 mg/mL was spin-coated at 4400 rpm onto PEDOT : PSS hole-injecting layer and then annealed at 120 °C for 10 min to afford a 30 nm thick film. The emitting layer was then overlaid by spin-coating at 2100 rpm using a filtered CH_2Cl_2 solution of mixed host and Ag_6Cu cluster complex (5.5 mg/mL). Subsequently, 50 nm of TPBi, 1 nm of LiF and 100 nm of Al were thermally deposited in an inert chamber at a base pressure less than 4×10^{-4} Pa. The electroluminescence (EL) spectra were recorded on OPT-2000 spectrophotometer. The current density-voltage-brightness (I-V-B) curves of the devices were recorded on a Keithley 2400/2000 source meter and a calibrated silicon photodiode. All measurements of the devices were carried out at ambient conditions.

Theoretical Calculation Methodology. The density functional theory (DFT) method[20] at the gradient-corrected correlation functional PBE1PBE level[21] was firstly used to optimize the geometrical structure of complex **1**. The input structure was extracted as an isolated molecule derived from experimentally determined geometry from the X-ray crystallographic data. The structure was fully optimized without considering any symmetry restriction. Then, based on the optimized geometrical structure, 100 singlet excited states were calculated to determine the vertical excitation energies by time-dependent DFT (TD-DFT) method.[22] The conductor-like polarizable continuum model method (CPCM)[23] using CH_2Cl_2 as the solvent was employed. In these calculations, the Lanl2dz[24] effective core potential was used to describe the inner electrons of Cu, Ag, and P atoms, while its associated double-ζ basis set of Hay and Wadt was employed for the remaining outer electrons with additional *f*- [Cu (α_f = 0.24), Ag (α_f = 0.22)] and *d*-type [P (α_d = 0.34)] polarization functions.[25] All-electron basis set of 6-31G(p,d) was used for other non-metal atoms of O, C, and H.[26] All the calculations were implemented using Gaussian 03 program package.[27] Visualization of the optimized structure and frontier molecular orbitals were performed by GaussView. Ros & Schuit method[28] (C-squared population analysis method, SCPA) is supported to analyze the partition orbital composition by using Multiwfn 2.4 program.[29]

Acknowledgements

This work was support from the 973 project from MSTC (2014CB845603), the NSF of China (21390392, 21473201, U1405252, 21531008 and 21303204), and the Natural Science Foundation of Fujian Province (2012J05034 and 2013J05036).

Notes and references

1 (a) C. Fan, C. Yang, Chem. Soc. Rev., 2014, 43, 6439; (b) P.-T. Chou, Y. Chi, *Chem. Eur. J*., 2007, **13**, 380; (c) G. Zhou, W.-Y. Wong, X. Yang, *Chem. Asian J*., 2011, **6**, 1706; (d) K. S. Yook, J. Y. Lee, *Adv. Mater.,* 2012, **24**, 3169.

2 (a) X. Wang, S.-L. Gong, D. Song, Z.-H. Lu, S. Wang, *Adv. Funct. Mater*., 2014, **24**, 7257; (b) X. Wang, Y.-L. Chang, J.-S. Lu, T. Zhang, Z.-H. Lu, S. Wang, *Adv. Funct. Mater*., 2014, **24**, 1911; (c) S.-L. Lai, W.-Y. Tong, S. C. F. Kui, M.-Y. Chan, C.-C. Kwok, C.-M. Che, *Adv. Funct. Mater.,* 2013, **23**, 5168; (d) X.-C. Hang, T. Fleetham, E. Turner, J. Brooks, J. Li, *Angew. Chem. Int. Ed*., 2013, **52**, 6753.

3 (a) M.-C. Tang, D. P.-K. Tsang, Y.-C. Wong, M.-Y. Chan, K. M.-C. Wong, V. W.-W. Yam, *J. Am. Chem. Soc*., 2014, **136**, 17861; (b) T. M. Dau, Y.-A. Chen, A. J. Karttunen, E. V. Grachova, S. P. Tunik, K.-T. Lin, W.-Y. Hung, P.-T. Chou, T. A. Pakkanen, I. O. Koshevoy, *Inorg. Chem*., 2014, **53**, 12720; (c) L.-J. Xu, J.-Y. Wang, X.-F. Zhu, X.-C. Zeng, Z.-N. Chen, *Adv. Funct. Mater*., 2015, **25**, 3033.

4 (a) T.-C. Lee, J.-Y. Hung, Y. Chi, Y.-M. Cheng, G.-H. Lee, P.-T. Chou, C.-C. Chen, C.-H. Chang, C.-C. Wu, *Adv. Funct. Mater*., 2009, **19**, 2639; (b) J.-L. Liao, Y. Chi, C.-C. Yeh, H.-C. Kao, C.-H. Chang, M.-A. Fox, P.-J. Low, G.-H. Lee, *J. Mater. Chem. C.,* 2015, **3**, 4910.

5 (a) Z.-K. Tan, R. S. Moghaddam, M. L. Lai, P. Docampo, R. Higler, F. Deschler, M. Price, A. Sadhanala, L. M. Pazos, D. Credgington, F. Hanusch, T. Bein, H. Snaith, R. H. Friend, *Nat.*

Nanotech., 2014, **9**, 687; (b) J. Wang, N. Wang. Y. Jin, J. Si, Z.-K. Tan, H. Du, L. Cheng, X. Dai, S. Bai, H. He, Z. Ye, M. L. Lai, R. H. Friend, W. Huang, *Adv. Mater*., 2015, **27**, 2311.

6 (a) G. Cheng, G. K.-M. So, W.-P. To, Y. Chen, C.-C. Kwok, C. Ma, X. Guan, X. Chang, W.-M. Kwoke, C.-M. Che, *Chem. Sci*., 2015, **6**, 4623. (b) Y. Sakai, Y. Sagara, H. Nomura, N. Nakamura, Y. Suzuki, H. Miyazakiae, C. Adachi, *Chem. Commun*., 2015, **51**, 3181.

7 (a) Y. Ma, C.-M. Che, H.-Y. Chao, X. Zhou, W.-H. Chan, J. Shen, *Adv. Mater.,* 1999, **11**, 852; (b) Q. Zhang, T. Komino, S. Huang, S. Matsunami, K. Goushi, C. Adachi, *Adv. Funct. Mater*., 2012, **22**, 2327; (c) Q. Zhang, Q. Zhou, Y. Cheng, L. Wang, D. Ma, X. Jing, F. Wang, *Adv. Mater*., 2004, **16**, 432; (d) F. Dumur, *Org. Electron.,* 2015, **21**, 27.

8 (a) C.-W. Hsu, C.-C. Lin, M.-W. Chung, Y. Chi, G.-H. Lee, P.-T. Chou, C.-H. Chang, P.-Y. Chen, *J. Am. Chem. Soc*., 2011, **133**, 12085; (b) J. C. Deaton, S. C. Switalski, D. Y. Kondakov, R. H. Young, T. D. Pawlik, D. J. Giesen, S. B. Harkins, A. J. M. Miller, S. F. Mickenberg, J. C. Peters, *J. Am. Chem. Soc*., 2010, **132**, 9499; (c) M. Hashimoto, S. Igawa, M. Yashima, I. Kawata, M. Hoshino, M. Osawa, *J. Am. Chem. Soc*., 2011, **133**, 10348.

9 (a) X. Liu, T. Zhang, T. Ni, N. Jiang, Z. Liu, Z. Bian, Z. Lu, C. Huang, *Adv. Funct. Mater*., 2014, **24**, 5385; (b) Z. Liu, J. Qiu, F. Wei, J. Wang, X. Liu, M. G. Helander, S. Rodney, Z. Wang, Z. Bian, Z. Lu, M. E. Thompson, C. Huang, *Chem. Mater*., 2014, **26**, 2368; (c) Z. Liu, M. F. Qayyum, C. Wu, M. T. Whited, P. I. Djurovich, K. O. Hodgson, B. Hedman, E. I. Solomon, M. E. |Thompson, *J. Am. Chem. Soc*., 2011, **133**, 3700; (d) D. M. Zink, D. Volz, T. Baumann, M. Mydlak, H. Flügge, J. Friedrichs, M. Nieger, S. Bräse, *Chem. Mater.,* 2013, **25**, 4471.

10 M. J. Leitl, V. A. Krylova, P. I. Djurovich, M. E. Thompson, H. Yersin, *J. Am. Chem. Soc*., 2014, **136**, 16032.

11 (a) Z.-H. Chen, L.-Y. Zhang, Z.-N. Chen, *Organometallics,* 2012, **31**, 256; (b) Q.-H. Wei, G.-Q. Yin, L.-Y. Zhang, L.-X. Shi, Z.-W. Mao, Z.-N. Chen, *Inorg. Chem*. 2004, **43**, 3484; (c) I. O. Koshevoy, A. J. Karttunen, Y.-C. Lin, C.-C. Lin, P.-T. Chou, S. P. Tunik, M. Haukka, T. Pakkanen, *Dalton Trans*., 2010, **39**, 2395.

12 (a) R. Czerwieniec, H. Yersin, *Inorg. Chem*., 2015, **54**, 4322; (b) H. Yersin, A. F. Rausch, R. Czerwieniec, T. Hofbeck, T. Fischer, *Coord. Chem. Rev*., 2011, **255**, 2622.

13 Y. Tao, K. Yuan, T. Chen, P. Xu, H. Li, R. Chen, C. Zheng, L. Zhang, W. Huang, *Adv. Mater*., 2014, **26**, 7931.

14 (a) X. Zhang, B. Li, Z.-H. Chen, Z.-N. Chen, *J. Mater. Chem*., 2012, **22**, 11427; (b) O. S. Wenger, *Chem. Rev*., 2013, **113**, 3686.

15 J. R. Shakirova, E. V. Grachova, A. S. Melnikov, V. V. Gurzhiy, S. P. Tunik, M. Haukka, T. A. Pakkanen, I.O. Koshevoy, *Organometallics*, **2013**, *32*, 4061.

16 (a) C. Monnereau, E. Blart, F. Odobel, *Tetrahedron Lett*., 2005, 5421; (b) S. Takahashi, Y. Kuroyama, K. Sonogashira, N. Hagihara, *Synth. Commun*., 1980, 627.

17 (a) D. C. Owsley, C. E. Castro, *Org. Synth.,* 1972, **52**, 128; (b) W. E. Hill, J. G. Taylor, C. A. McAuliffe, K. W. Muir, L. M. Muir, *J. Chem. Soc., Dalton Trans.,* 1982, 833.

18 J. N. Demasa, G. A. Crosby, *J. Phys. Chem.,* 1971, **75**, 991.

19 G. M. Sheldrick, *SHELXL-97*, *Program for the Refinement of Crystal Structures*; University of Göttingen: Göttingen, Germany, **1997**.

20 A. D. Becke, *J. Chem. Phys.,* 1993, **98**, 5648.

21 J. P. Perdew, K. Burke, M. Ernzerhof, *Phys. Rev. Lett.,* 1996, **77**, 3865.

22 (a) M. E. Casida, C. Jamorski, K. C. Casida, D. R. Salahub, *J. Chem. Phys.,* 1998, **108**, 4439; (b) R. E. Stratmann, G. E. Scuseria, M. J. Frisch, *J. Chem Phys.,* 1998, **109**, 8218; (c) R. Bauernschmitt, R. Ahlrichs, *Chem. Phys. Lett.,* 1996, **256**, 454.

23 M. Cossi, N. Rega, G. Scalmani, V. Barone, *J. Comput*. *Chem*., 2003, **24**, 669.

24 (a) P. J. Hay, W. R. Wadt, *J. Chem. Phys.,* 1985, **82**, 270; (b) W. R. Wadt, P. J. Hay, *J. Chem. Phys.,* 1985, **82**, 284.

25 P. J. Hay, W. R. Wadt, *J. Chem. Phys*. 1985, **82**, 299.

26 M. M. Francl, W. J. Pietro, W. J. Hehre, J. S. Binkley, M. S. Gordon, D. J. DeFrees, J. A. Pople, *J. Chem. Phys*., 1982, **77**, 3654.

27 M. J., Frisch, G. W. Trucks, H. B. Schlegel, G. E. Scuseria, M. A. Robb, J. R. Cheeseman, J. A., Montgomery, Jr., T.Vreven, K. N. Kudin, J. C. Burant, J. M. Millam, S. S. Iyengar, J. Tomasi, V. Barone, B. Mennucci, M. Cossi, G. Scalmani, N. Rega, G. A. Petersson, H. Nakatsuji, M. Hada, M. Ehara, K. Toyota, R. Fukuda, J. Hasegawa, M. Ishida, T. Nakajima, Y. Honda, O. Kitao, H. Nakai, M. Klene, X. Li, J. E. Knox, H. P. Hratchian, J. B. , V. Bakken, C. Adamo, J. Jaramillo, R. Gomperts, R. E. Stratmann, O. Yazyev, A. J. Austin, R. Cammi, C. Pomelli, J. W. Ochterski, P. Y. Ayala, K. Morokuma, G. A. Voth, P. Salvador, J. J. Dannenberg, V. G. Zakrzewski, S. Dapprich, A. D. Daniels, M. C. Strain, O. Farkas, D. K. Malick, A. D. Rabuck, K. Raghavachari, J. B. Foresman, J. V. Ortiz, Q. Cui, A. G. Baboul, S. Clifford, J. Cioslowski, B. B. Stefanov, G. Liu, A. Liashenko, P. Piskorz, I. Komaromi, R. L. Martin, D. J. Fox, T. Keith, M. A. Al-Laham, C. Y. Peng, A. Nanayakkara, M. Challacombe, P. M. W. Gill, B. Johnson, W. Chen, M. W. Wong, C. Gonzalez, J. A. Pople, *Gaussian 03, revision D.02.* Gaussian, Inc.: Wallingford, CT, 2004.

28 P. Ros, G. C. A. Schuit, *Theo. Chim. Acta (Berl.)*, 1966, **4**, 1.

29 T. Lu, F. W. Chen, *J. Comp*. *Chem*., 2012, **33**, 580.

Title: Highly Efficient Phosphorescence and Electroluminescence of Cationic Copper(I)-Silver(I) Heterometallic Cluster Complexes

Authors: Liang-Jin Xu, Xu Zhang, Jin-Yun Wang and Zhong-Ning Chen*

Strongly phosphorescent cationic Ag_6Cu cluster complexes show highly efficient electroluminescence from solution-processed OLEDs with current efficiency of 42.5 cd/A and external quantum efficiency of 13.9% at a low bias voltage (4.5 V).